REPORTS

SUPERCONDUCTIVITY

Observation of superconductivity in hydrogen sulfide from nuclear resonant scattering

Ivan Troyan,[1,2]*† Alexander Gavriliuk,[2,3]† Rudolf Rüffer,[4] Alexander Chumakov,[4,5] Anna Mironovich,[3] Igor Lyubutin,[2] Dmitry Perekalin,[6] Alexander P. Drozdov,[1] Mikhail I. Eremets[1]

High-temperature superconductivity remains a focus of experimental and theoretical research. Hydrogen sulfide (H_2S) has been reported to be superconducting at high pressures and with a high transition temperature. We report on the direct observation of the expulsion of the magnetic field in H_2S compressed to 153 gigapascals. A thin ^{119}Sn film placed inside the H_2S sample was used as a sensor of the magnetic field. The magnetic field on the ^{119}Sn sensor was monitored by nuclear resonance scattering of synchrotron radiation. Our results demonstrate that an external static magnetic field of about 0.7 tesla is expelled from the volume of ^{119}Sn foil as a result of the shielding by the H_2S sample at temperatures between 4.7 K and approximately 140 K, revealing a superconducting state of H_2S.

High-temperature superconductivity at high pressures has been predicted for numerous hydrides (*1*–*7*), including H_2S (*8*, *9*). Recent resistivity and magnetic susceptibility measurements indicate that a superconducting transition occurs in H_2S compressed to between 150 and 190 GPa with a high onset temperature of 203 K (*10*). For an unambiguous identification of the superconducting state, a direct observation of the Meissner effect in an external magnetic field is desirable. However, measurements of the Meissner effect using a superconducting quantum interference device (SQUID) or inductor methods at pressures above 130 GPa are difficult, and experimental results do not allow for a clear interpretation.

Historically, the Meissner effect was defined as the expulsion of the external magnetic field from a superconducting sample as the sample enters the superconducting state with decreasing temperature—that is, upon field cooling (FC) conditions. In our experiment, the sample was first transformed into the superconducting state upon zero field cooling (ZFC), and then the external magnetic field was applied. Upon warming the sample, we monitored the expulsion of the magnetic flux in the diamagnetic shielding mode. Relative to the FC option, the ZFC protocol is a better choice for high-temperature superconductors because this method provides a larger contrast in measurements of the expulsion of the magnetic field (*11*). To detect the expulsion of the magnetic field, we used a magnetic field sensor immersed into the H_2S specimen (Fig. 1). A 2.6-μm-thick foil of tin enriched with the ^{119}Sn isotope to 95% was used as the sensor. It was placed in the gasket hole of the diamond anvil cell (DAC) before loading H_2S. The sensor monitored the magnetic field via the magnetic interaction at the ^{119}Sn nucleus, as detected by nuclear resonance scattering (NRS) of synchrotron radiation (*12*, *13*). The presence of the magnetic field at tin nuclei was identified by quantum beats in the time spectra of NRS (*14*). The resonant character of NRS ensured that we acquired data only from the ^{119}Sn sensor, with zero background from the sample environment.

[1]Max-Planck-Institut für Chemie, 55020 Mainz, Germany. [2]Shubnikov Institute of Crystallography, Russian Academy of Sciences, Moscow 119333, Russia. [3]Institute for Nuclear Research, Russian Academy of Sciences, Troitsk, Moscow 142190, Russia. [4]European Synchrotron Radiation Facility, CS40220, F-38043 Grenoble Cedex 9, France. [5]National Research Center "Kurchatov Institute," 123182 Moscow, Russia. [6]A. N. Nesmeyanov Institute of Organoelement Compounds, Russian Academy of Sciences, Moscow 119991, Russia.
*Corresponding author. E-mail: itrojan64@gmail.com
†These authors contributed equally to this work.

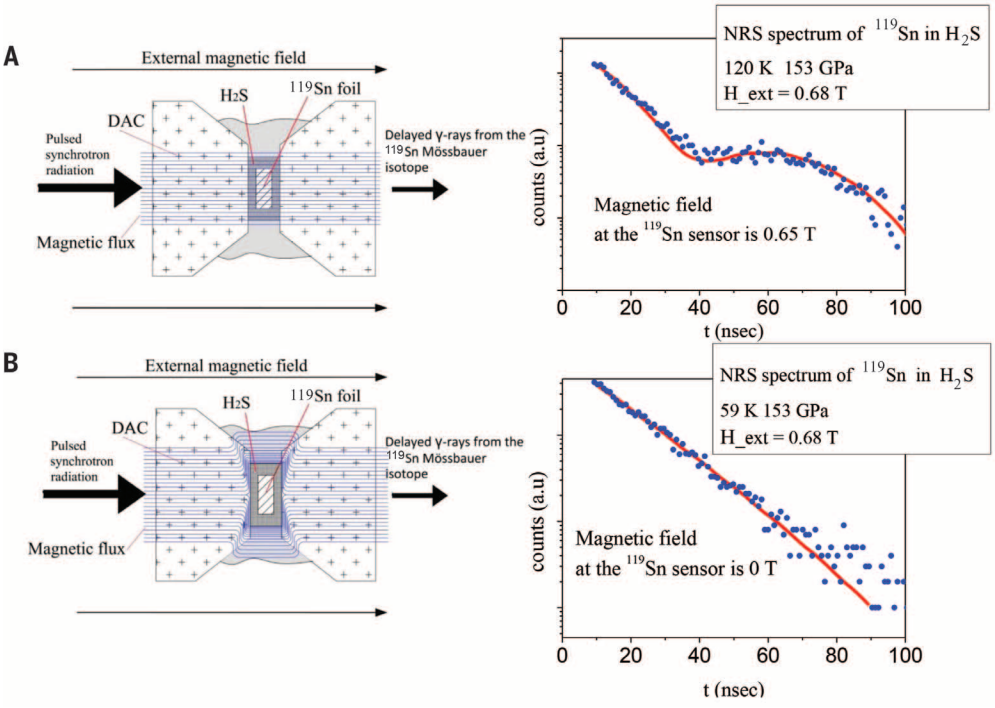

Fig. 1. Layout of the experiment. The tin foil, surrounded by compressed hydrogen sulfide, is located in a diamond anvil cell (DAC) at a pressure of about 153 GPa. Pulsed synchrotron radiation excites the nuclei of the tin Mössbauer isotope ^{119}Sn. The detection system measures the time evolution of radiation emitted by the tin nuclei in the forward direction. (**A**) At $T > T_c$, in the external magnetic field directed along the x-ray beam, the time spectra show quantum beats due to magnetic splitting of tin nuclear levels. (**B**) At $T < T_c$, the tin foil is screened from the external magnetic field by the superconducting hydrogen sulfide, and consequently no splitting of nuclear levels occurs and no magnetic quantum beats are seen in the time spectra. The blue dots are experimental data; the red lines were obtained from fits using the MOTIF software (*17*).

For sample preparation, we followed the procedure described in (*10*). The gaseous H_2S was filled into the DAC through a capillary system in an optical cryostat that enabled in situ pressure changes in the DAC. The filling started after the temperature had been decreased to 197 K. The ^{119}Sn foil was immersed in liquid H_2S in the hole inside the gasket of the DAC (Fig. 2A). The H_2S sample was identified by Raman scattering (Fig. 2A, bottom). The value of the pressure was measured by Raman scattering from the diamond anvils (*15*, *16*).

The DAC was installed into the cryo-magnet system with exchange gas cooling. To verify that superconductivity occurred in the studied H_2S sample and not in the sensor ^{119}Sn foil, we conducted the measurements simultaneously with two DACs. One DAC contained the H_2S sample and the ^{119}Sn sensor foil, and the other contained the reference ^{119}Sn foil loaded with hydrogen (H_2) as a pressure-transmitting medium (Fig. 2C and fig. S1). The samples in both DACs were maintained under the same magnetic field and temperature conditions. The alternating position of each DAC relative to the x-ray beam spot was performed by vertical motion of the sample insert (fig. S1). For a cross-check of data reliability, the measurements were performed using two cryomagnet systems with different directions of the external magnetic field: one for the horizontal field directed along the x-ray beam, and another for the vertical field perpendicular to the x-ray beam. The measuring procedure was as follows: First, the sample was cooled in zero magnetic field down to the lowest temperature of 5 K. Then, a magnetic field of about 0.7 T was applied. The exact values of the external field were derived from the measurements with the reference foil (*11*) as 0.68 T and 0.65 T for the magnetic field perpendicular and parallel to the sample plane, respectively. After that, the NRS spectra were recorded at each temperature point while the temperature was increased.

In the superconducting state of H_2S, an external magnetic field applied perpendicular to the sample did not penetrate to the ^{119}Sn foil (fig. S6). Therefore, the ^{119}Sn nuclear ground (nuclear spin I_g = 1/2) and excited (I_{ex} = 3/2) levels are not split. The corresponding time spectra show an exponential decay (Fig. 1B). When the superconducting state is partially destroyed, the magnetic field penetrates into the sample volume, and the nuclear levels of ^{119}Sn become split by the external magnetic field. For split levels, NRS (*14*) involves several radiation components with different energies. Their interference leads to the quantum beats in the time dependence of nuclear decay, and the beat period is inversely proportional to the splitting of the nuclear levels. In the time window available in our measurements, the quantum beats are observed by the appearance of the first beat minimum (Fig. 1A), with the position inversely proportional to the value of magnetic field at the ^{119}Sn nuclei. The exact data of the observed magnetic fields at tin nuclei were obtained by the theoretical fit to the experimental data points [red line in Fig. 1A; see (*11*, *17*) for details].

Figure 3, A and B, shows the results obtained with an external magnetic field of 0.68 T applied along the x-ray beam (i.e., perpendicular to the sample plane). In the range of 4.7 to 59 K, the NRS spectra show an exponential decay, which demonstrates that the magnetic field is completely expelled from the sensor. The screening of the magnetic field at the ^{119}Sn sensor is due to the expulsion of the field in a superconducting H_2S. At and above 100 K, quantum beats appear, indicating that the external magnetic field starts penetrating into the sensor foil. The penetration of the magnetic field inside the ^{119}Sn foil increases gradually above 100 K. However, even for the data point at 120 K, the magnetic field on the sensor still does not reach the value of the external magnetic field (Figs. 3A and 4A). This demonstrates that the partial screening still remains up to at least 120 K. The sample is in the mixed superconducting state, and the amount of the samples in the normal state increases with temperature.

The distributions of magnetic flux at different magnetic field directions for a finite-size superconducting sample have been carefully investigated theoretically (*18*–*20*). The calculations show that the effect of strong expulsion of perpendicular magnetic field from the central part of a finite-size type II superconductor could be observed even if the first critical field is lower than the external magnetic field.

In contrast to the case of the H_2S sample, the measurements of the reference sample showed the quantum beats even at the lowest temperatures (Fig. 3B). This confirmed that the reference ^{119}Sn foil is not in a superconducting state; therefore, the observed expulsion of the magnetic field is associated only with the superconducting H_2S.

A similar trend was observed when an external magnetic field of 0.65 T was applied vertically (i.e., parallel to the sample plane) (Fig. 3, C and D), although this case is more complicated because of the less favorable conditions of screening (*11*). For all temperatures, the fit of the NRS spectra for the H_2S sample (Fig. 3C) reveals a superposition of states with the zero and finite

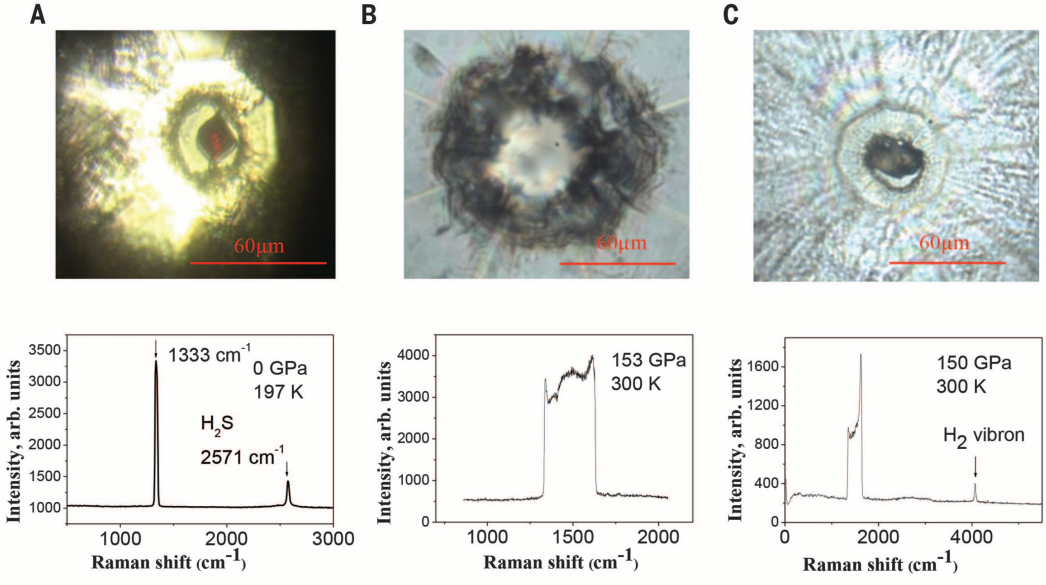

Fig. 2. Experimental mounts. (**A**) Top: Tin foil sensor (seen as a black square) immersed in liquefied hydrogen sulfide in the just-clamped DAC at pressures near ambient. The photo in transmitted light was taken in a special cryostat designed for the cryogenic filling DAC. The H_2S sample size is approximately 30 μm. Bottom: The Raman spectrum measured when filling liquefied hydrogen sulfide into DAC. The Raman line of diamond (1333 cm^{-1}) and the hydrogen sulfide vibron (2571 cm^{-1}) are clearly visible in the spectrum. (**B**) Top: Hydrogen sulfide at pressure of 153 GPa. The central well-reflecting part is the superconducting phase of H_2S. The tin foil is located inside the superconducting sample. Bottom: The Raman spectrum from the surface of the diamond anvil taken over the central part is broadened by the pressure in the chamber. The right sharp edge of the spectrum indicates good hydrostatic conditions in the sample. This spectrum was used to measure pressure during the experiment. (**C**) Top: The reference DAC. The central dark object is the tin foil in hydrogen at a pressure of 150 GPa. The ^{119}Sn sample size is about 20 to 35 μm. Bottom: The Raman spectrum contains the broadened line of the diamond anvils and the hydrogen vibron.

magnetic field. This suggests that the field can partially penetrate into the sensor. In addition, this effect can appear if the H_2S sample is mixed with the material of the gasket at the boundary of the gasket hole, and the sample H_2S is a type II superconductor. This allows the magnetic field parallel to the surface of the anvil to penetrate into the ^{119}Sn foil. The value of the average magnetic field inside H_2S as a function of temperature is shown in Fig. 4B. The increase of penetration of the external magnetic field into the sensor foil occurred at about 100 K. This is the same temperature near which the transition was observed with a perpendicular magnetic field (Fig. 4A). Above 100 K, the fraction of the samples in the normal state increased with temperature. However, even for the data point at 145 K, the magnetic field on the sensor still did not reach the value of the external magnetic field (Figs. 3C and 4B). This shows that the partial screening still remains at least up to 145 K. In contrast, the NRS spectra measured for the reference ^{119}Sn foil reveal the absence of the superconducting state for all temperatures (Fig. 3D). Additionally, this

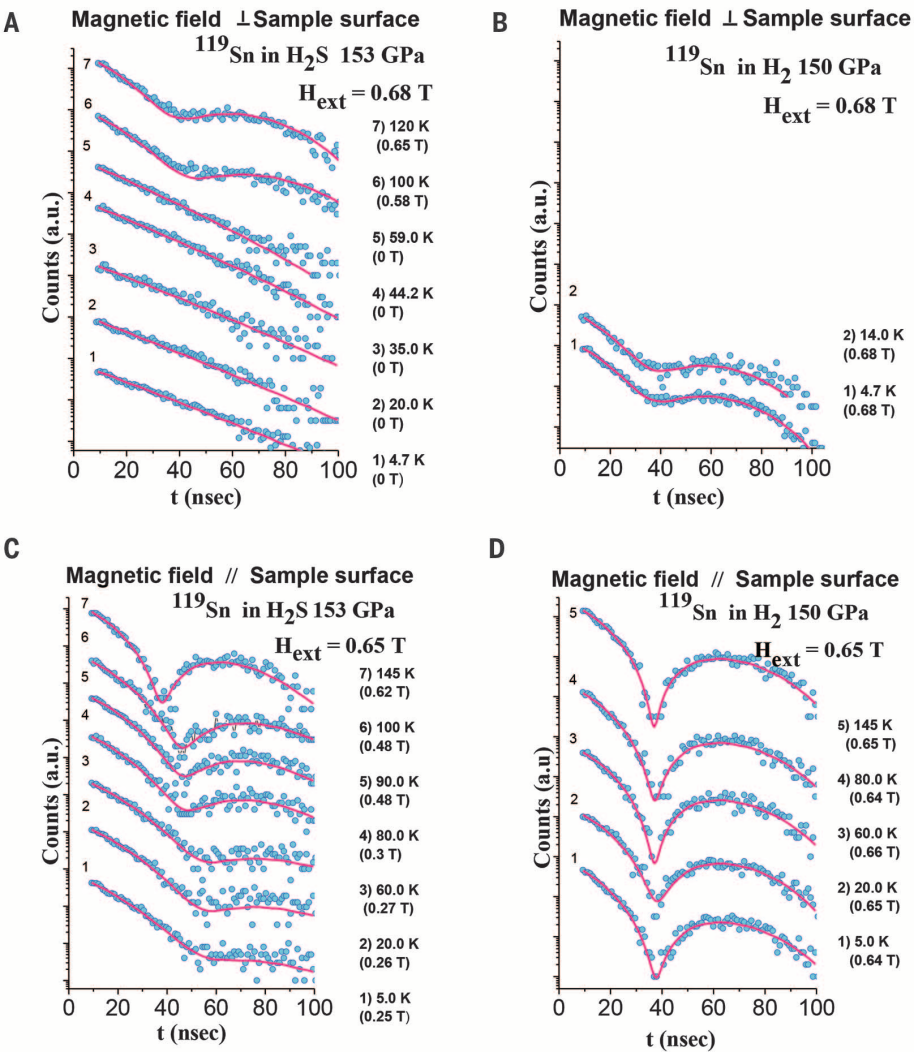

Fig. 3. Experimental NRS spectra. The time NRS spectra from ^{119}Sn in H_2S at 153 GPa (left panels) and in H_2 at 150 GPa (right panels) in an external magnetic field in the horizontal (top) and vertical (bottom) field geometry. Dots (blue) are the experimental data; solid lines (red) are the fits by the MOTIF software (*17*). Temperatures of the samples and the values of magnetic fields at the ^{119}Sn nuclear site obtained from the fits are shown to the right of the corresponding NRS spectra. (**A**) Temperature evolution of the NRS spectra from ^{119}Sn in H_2S at pressure of 153 GPa and magnetic field of 0.68 T (horizontal) between 4.7 and 120 K. The pure exponential decay shown in curves 1 to 5 indicates that no magnetic field is present at the ^{119}Sn nuclear sites. This proves that the external magnetic field cannot penetrate through H_2S, hence it is a superconductor (expulsion of the magnetic field). At 100 K, pronounced oscillations (quantum beats) start to develop, revealing the occurrence of a magnetic field at the sensor. (**B**) Temperature evolution of the NRS spectra in the reference sample ^{119}Sn in H_2 at 150 GPa and magnetic field of 0.68 T (horizontal) at 4.7 and 14 K. The quantum beats reveal the presence of a magnetic field at the sensor. (**C**) Temperature evolution of the NRS spectra of ^{119}Sn in H_2S at 153 GPa and magnetic field of 0.65 T (vertical) between 5 and 145 K. As temperature increases, the slowly developing quantum beats indicate the decreasing screening of the external magnetic field by the superconductor. (**D**) Temperature evolution of the NRS spectra of the reference sample ^{119}Sn in H_2 at 150 GPa and magnetic field of 0.65 T (vertical) between 5 and 145 K. The quantum beats reveal the presence of a magnetic field.

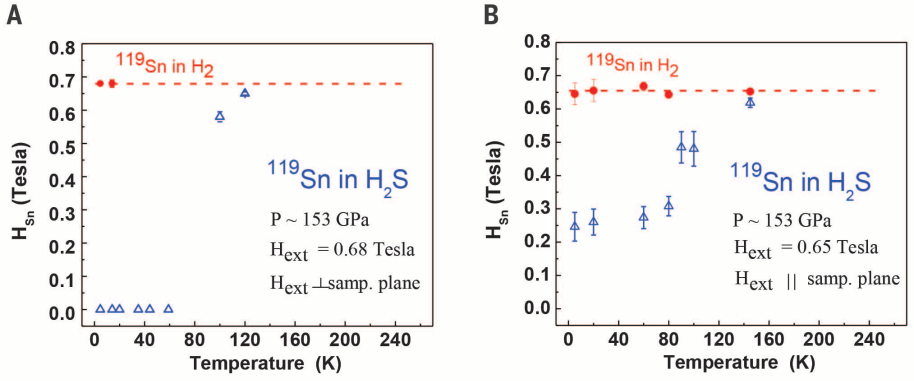

Fig. 4. Influence of temperature on magnetic field inside H_2S. The temperature dependence of the magnetic field was determined from the NRS spectra of the ^{119}Sn sensor inside H_2S at 153 GPa (blue triangles) and the field at the reference sample ^{119}Sn in H_2 at 150 GPa (red dots). (**A** and **B**) Measurements in the horizontal and vertical geometry of the external magnetic field, respectively. Dashed lines are guides to the eye. Some error bars are smaller than the size of the symbols.

confirms that the observed superconductivity of the studied sample is related entirely to H_2S.

Our results demonstrate that the superconducting H_2S sample effectively shields the strong magnetic field of about 0.7 T up to temperatures of 90 to 100 K. The partial shielding of the magnetic field persists up to about 140 K. This confirms that H_2S compressed to 150 GPa is the superconductor with the very high critical parameters. Referring to data given in (*10*), it should be noted that the resistivity measurements rely on the very onset of the current percolation, whereas the magnetic measurements require a somewhat larger amount of the sample to be transformed to the superconducting phase.

REFERENCES AND NOTES

1. N. W. Ashcroft, *Phys. Rev. Lett.* **92**, 187002 (2004).
2. J. Feng *et al.*, *Phys. Rev. Lett.* **96**, 017006 (2006).
3. G. Gao *et al.*, *Phys. Rev. Lett.* **101**, 107002 (2008).
4. D. Y. Kim, R. H. Scheicher, H. K. Mao, T. W. Kang, R. Ahuja, *Proc. Natl. Acad. Sci. U.S.A.* **107**, 2793–2796 (2010).
5. G. Gao *et al.*, *Proc. Natl. Acad. Sci. U.S.A.* **107**, 1317–1320 (2010).
6. D. Y. Kim, R. H. Scheicher, C. J. Pickard, R. J. Needs, R. Ahuja, *Phys. Rev. Lett.* **107**, 117002 (2011).
7. H. Wang, J. S. Tse, K. Tanaka, T. Iitaka, Y. Ma, *Proc. Natl. Acad. Sci. U.S.A.* **109**, 6463–6466 (2012).
8. D. Duan *et al.*, *Sci. Rep.* **4**, 6968 (2014).
9. Y. Li, J. Hao, H. Liu, Y. Li, Y. Ma, *J. Chem. Phys.* **140**, 174712 (2014).
10. A. P. Drozdov, M. I. Eremets, I. A. Troyan, V. Ksenofontov, S. I. Shylin, *Nature* **525**, 73–76 (2015).
11. See supplementary materials on *Science* Online.
12. I. S. Lyubutin, T. V. Dmitrieva, *JETP Lett.* **21**, 59 (1975).
13. E. Gerdau, H. de Waard, *Nuclear Resonant Scattering of Synchrotron Radiation*, vol. 123–124 of *Hyperfine Interactions* (Springer, 1999), pp. 1–2.
14. J. B. Hastings, D. P. Siddons, U. van Bürck, R. Hollatz, U. Bergmann, *Phys. Rev. Lett.* **66**, 770–773 (1991).
15. N. Dubrovinskaia, L. Dubrovinsky, R. Caracas, M. Hanfland, *Appl. Phys. Lett.* **97**, 251903 (2010).
16. Y. Akahama, H. Kawamura, *J. Phys. Conf. Ser.* **215**, 012195 (2010).
17. Y. V. Shvyd'ko, *Phys. Rev. B* **59**, 9132–9143 (1999).
18. E. H. Brandt, *Phys. Rev. B* **54**, 4246–4264 (1996).
19. E. H. Brandt, *Phys. Rev. B* **58**, 6506–6522 (1998).
20. G. P. Mikitik, E. H. Brandt, M. V. Indenbom, *Phys. Rev. B* **70**, 014520 (2004).

ACKNOWLEDGMENTS

The high-pressure samples of hydrogen sulfide and hydrogen investigated in this study have been prepared using the techniques and equipment designed and built by M.I.E. and A.P.D. Funding was provided by the European Research Council (ERC Advanced Grant 267777 of M.I.E.) and the Max Planck Institute for Chemistry, Mainz. This work was also supported by Russian Science Foundation grant 14-12-00848 (I.T., A.G., and I.L.), Russian Foundation for Basic Research grant 14-02-00483-a (A.G.), and the Russian Academy of Sciences program "Physics of elementary particles, fundamental nuclear physics and nuclear technologies."

SUPPLEMENTARY MATERIALS

www.sciencemag.org/content/351/6279/1303/suppl/DC1
Materials and Methods
Supplementary Text
Figs. S1 to S6
References (*21*–*24*)

17 June 2015; accepted 4 January 2016
10.1126/science.aac8176

NANOMATERIALS

Formation of pseudomorphic nanocages from Cu_2O nanocrystals through anion exchange reactions

Hsin-Lun Wu, Ryota Sato, Atsushi Yamaguchi, Masato Kimura, Mitsutaka Haruta, Hiroki Kurata, Toshiharu Teranishi*

The crystal structure of ionic nanocrystals (NCs) is usually controlled through reaction temperature, according to their phase diagram. We show that when ionic NCs with different shapes, but identical crystal structures, were subjected to anion exchange reactions under ambient conditions, pseudomorphic products with different crystal systems were obtained. The shape-dependent anionic framework (surface anion sublattice and stacking pattern) of Cu_2O NCs determined the crystal system of anion-exchanged products of Cu_xS nanocages. This method enabled us to convert a body-centered cubic lattice into either a face-centered cubic or a hexagonally close-packed lattice to form crystallographically unusual, multiply twinned structures. Subsequent cation exchange reactions produced CdS nanocages while preserving the multiply-twinned structures. A high-temperature stable phase such as wurtzite ZnS was also obtained with this method at ambient conditions.

Chemical conversion of semiconductor nanocrystals (NCs) via ion-exchange reactions can overcome the difficulties associated with controlling the size, shape, chemical composition, and crystal structure in conventional syntheses (*1*–*7*). However, the crystal structure transformation in ion-exchange reactions is still not well understood. When the entire crystal is in a structurally nonequilibrium state in ion-exchange reactions, both the cations and anions are mobile and can induce morphological changes to the thermodynamically more stable shape before reaching the final equilibrium state. For ionic NCs above a critical size, the anion framework remains intact, and the original shape of the parent NCs is retained throughout the cation-exchange reaction (*8*). The retained shape of the parent NCs in ion exchange provides an opportunity to obtain nonequilibrium distinct structures and even new structures of ionic NCs (*9*)—these final structures being known as "pseudomorphs."

We show, using Cu_2O NCs with well-defined shapes as parent NCs (*10*, *11*), a distinctive shape-dependent anionic frameworks–induced crystal phase transition in anion-exchange reaction at ambient conditions. Regular hexahedral (RH) Cu_2O NCs with a cubic phase were converted into RH $Cu_{1.8}S$ nanocages with a cubic phase, whereas rhombic dodecahedral (RD) Cu_2O NCs with a cubic phase were converted into RD $Cu_{1.75}S$ nanocages with a triclinic phase (*12*) after partial anion-exchange reaction. The Cu_2O NCs have a body-centered cubic (bcc) anion sublattice, but they were converted into the Cu_xS nanocages with either a face-centered cubic (fcc) or a hexagonally close-packed (hcp) anion sublattice.

Institute for Chemical Research, Kyoto University, Gokasho, Uji, Kyoto 611-0011, Japan.
*Corresponding author. E-mail: teranisi@scl.kyoto-u.ac.jp

Furthermore, shape retention of the Cu_xS pseudomorphic nanocages after the Cu_2O NCs provided new multiply twinned structures consisting of unusual connections between crystallographically independent walls. Subsequent cation-exchange reactions performed on RH and RD Cu_xS nanocages produced RH and RD CdS nanocages with a zincblende and a wurtzite phase, respectively, and preserved the pseudomorphic structures. The wurtzite ZnS nanocages, which formed under ambient conditions, are much more desirable for their optical properties than are the zincblende phases (*13*, *14*), which are usually synthesized at ~600°C (*15*).

Scanning electron microscopy (SEM) images, x-ray diffraction (XRD), and ultraviolet–visible–near infrared (UV-Vis-NIR) spectra of the Cu_2O NCs and the Cu_xS and CdS pseudomorphic nanocages are shown in Fig. 1. All reactions were performed under ambient conditions (*16*). Partial anion-exchange reactions of the RH and RD Cu_2O NCs (Fig. 1, A to C) with Na_2S gave cubic RH $Cu_{1.8}S$ and triclinic RD $Cu_{1.75}S$ nanocages (Fig. 1, D and E). The characteristic UV-Vis-NIR spectra of the products (Fig. 1F) confirmed that they were indeed Cu_xS nanocages (*17*). Subsequent cation exchange of RH $Cu_{1.8}S$ nanocages with Cd^{2+} generated the zincblende RH CdS as majority (Fig. 1, G and H). More accurately, the XRD pattern (Fig. 1H) reflects the large amount of twinning in the RH nanocages, and heavily twinned fcc shows up as hcp. On the other hand, the cation exchange of RD $Cu_{1.75}S$ nanocages with Cd^{2+} generated the wurtzite RD CdS nanocages. The UV-Vis-NIR spectra displayed the characteristic semiconducting CdS phase (Fig. 1I). Low-magnification SEM images of the Cu_xS and CdS nanocages are presented in fig. S1.

The overall phase transitions starting from the RH and RD Cu_2O NCs are illustrated schematically in Fig. 2. The RH Cu_2O NCs, which were

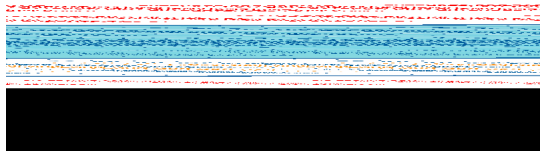

Observation of superconductivity in hydrogen sulfide from nuclear resonant scattering
Ivan Troyan, Alexander Gavriliuk, Rudolf Rüffer, Alexander Chumakov, Anna Mironovich, Igor Lyubutin, Dmitry Perekalin, Alexander P. Drozdov and Mikhail I. Eremets (March 17, 2016)
Science **351** (6279), 1303-1306. [doi: 10.1126/science.aac8176]

Editor's Summary

Peeking into a diamond pressure cell

A defining characteristic of a superconductor is that it expels an external magnetic field. Demonstrating this effect can be tricky when the sample is under enormous pressures in a diamond anvil cell. Troyan *et al.* placed a tinfoil sensor inside a sample of H_2S under pressure. They then bombarded it with synchrotron radiation and watched how the scattering of photons of tin nuclei changed over time. When H_2S was in the normal state, an external magnetic field reached the sensor through the sample, causing the nuclear levels of tin to split. In the superconducting state, however, no splitting was observed because H_2S expelled the field before it could reach the sensor.

Science, this issue p. 1303

Science (print ISSN 0036-8075; online ISSN 1095-9203) is published weekly, except the last week in December, by the American Association for the Advancement of Science, 1200 New York Avenue NW, Washington, DC 20005.